Membrane-Aerated Microbioreactor for High-Throughput Bioprocessing

Andrea Zanzotto,[1] Nicolas Szita,[1] Paolo Boccazzi,[2] Philip Lessard,[2] Anthony J. Sinskey,[2] Klavs F. Jensen[1]

[1]Department of Chemical Engineering, Massachusetts Institute of Technology, Cambridge, Massachusetts 02139; telephone: +1 (617) 253-4589; fax: +1 (614) 258-8224; e-mail: kfjensen@mit.edu
[2]Department of Biology, Massachusetts Institute of Technology, Cambridge, Massachusetts 02139

Received 16 December 2003; accepted 19 March 2004

Published online 21 June 2004 in Wiley InterScience (www.interscience.wiley.com). DOI: 10.1002/bit.20140

Abstract: A microbioreactor with a volume of microliters is fabricated out of poly(dimethylsiloxane) (PDMS) and glass. Aeration of microbial cultures is through a gas-permeable PDMS membrane. Sensors are integrated for on-line measurement of optical density (OD), dissolved oxygen (DO), and pH. All three parameter measurements are based on optical methods. Optical density is monitored via transmittance measurements through the well of the microbioreactor while dissolved oxygen and pH are measured using fluorescence lifetime-based sensors incorporated into the body of the microbioreactor. Bacterial fermentations carried out in the microbioreactor under well-defined conditions are compared to results obtained in a 500-mL bench-scale bioreactor. It is shown that the behavior of the bacteria in the microbioreactor is similar to that in the larger bioreactor. This similarity includes growth kinetics, dissolved oxygen profile within the vessel over time, pH profile over time, final number of cells, and cell morphology. Results from off-line analysis of the medium to examine organic acid production and substrate utilization are presented. By changing the gaseous environmental conditions, it is demonstrated that oxygen levels within the microbioreactor can be manipulated. Furthermore, it is demonstrated that the sensitivity and reproducibility of the microbioreactor system are such that statistically significant differences in the time evolution of the OD, DO, and pH can be used to distinguish between different physiological states. Finally, modeling of the transient oxygen transfer within the microbioreactor based on observed and predicted growth kinetics is used to quantitatively characterize oxygen depletion in the system.

Keywords: microbioreactor; oxygen sensor; pH sensor; oxygen transfer; screening; bioprocess development

INTRODUCTION

The number and variety of products obtained through microbial fermentation today is large and growing quickly. These products include, among others, primary metabolites, secondary metabolites, enzymes, therapeutic proteins, vaccines, and gums (Schmid and Hammelehle, 2003). Each new product is the result of a development process that begins at the screening stage (Gram, 1997; Shanks and Stephanopoulos, 2000). During this phase, many potential bacterial strains are screened to identify those that have the most favorable yield of the desired product. Criteria at this stage may be a high yield on a specific substrate or high production under certain growth conditions. The screening phase may be combined with strain optimization using techniques of metabolic engineering, in which case strain creation and screening are carried out iteratively (Chartrain et al., 2000; Parekh et al., 2000). Experiments at the screening phase are typically carried out using a combination of Petri dishes, microtiter plates, and shake flasks. Once a likely microbial candidate has been identified, the strain is transferred to the development phase. At this stage, the physiology of the strain is characterized in more detail, and the growth conditions of the strain are determined. These experiments are generally carried out in bioreactors with volumes of 0.5–10 L. From here, development proceeds as the process is gradually scaled up in bioreactor volume until production scale is reached (100,000–300,000 L).

Significant limitations in data generation currently exist at every stage of microbial and process development. During the screening phase, only limited control of environmental parameters is possible, and endpoint data are generally obtained to gauge the performance of cells. Efforts have been made to overcome this limitation. In microtiter plates, on-line measurements of dissolved oxygen (Stitt et al., 2002; John et al., 2003b) and pH (John et al., 2003a) during fermentation have been demonstrated. On-line measurements of dissolved oxygen (Anderlei and Buchs, 2001; Tolosa et al., 2002; Gupta and Rao, 2003; Wittmann et al., 2003) and pH (Weuster-Botz et al., 2001) in shake flasks during fermentation have also been reported. However, these screening approaches have the fundamental limitation that

Correspondence to: Klavs F. Jensen
Contract grant sponsors: DuPont–MIT Alliance (DMA); Swiss National Foundation

the effort involved largely continues to scale with the number of individual cultures involved, meaning that experiments with more cultures become more demanding both technically and mechanically. This is exacerbated by the difficulty of integrating culture steps that precede and follow the fermentation itself. During the process development phase that follows, the prohibitive time, expense, and labor involved in running experiments limit the number of strains and conditions that can be tested. At each stage, therefore, decisions are made with incomplete and insufficient data sets. A need clearly exists for a bioprocessing platform that would allow high-throughput, parallel, automated processing of a variety of bacterial strains under a variety of controlled conditions, with integrated sensors yielding real-time data on process parameters.

Efforts in this area have been made. Kim and Lee (1998) developed a silicon microfermenter chip that makes use of electrodes to measure cell density, dissolved oxygen, pH, and glucose. However, cell growth was not reported. Kostov et al. (2001) described a 2-mL microbioreactor that consists of a cuvette equipped with optical sensors for the continuous measurement of optical density, dissolved oxygen, and pH, in which aeration is accomplished by sparging the medium with air. Maharbiz et al. (2003, 2004) developed a bioreactor using microtiter plate wells, integrated with an aeration system in which oxygen is generated beneath a silicone membrane using hydrolysis. Biomass is measured optically, and pH is monitored using a solid-state pH sensor chip. Oxygen input rates are also monitored. The volume of this bioreactor is approximately 250 μL. Lamping et al. (2003) reported on a miniature bioreactor machined from Plexiglas with a working volume of 6 mL. Oxygenation in this bioreactor is achieved by sparging, and mixing is achieved by means of an impeller. Measurements of cell density, dissolved oxygen, and pH are performed optically.

We have developed a membrane-aerated microbioreactor with a volume as low as 5 μL. The size and design of the microbioreactor are compatible with microfabrication techniques, which enable fast and inexpensive scale-out through multiplication of devices. A microfabricated bioprocessing platform also allows integration of sensors as well as automation of liquid handling and process control. In this work, we describe the design and fabrication of the microbioreactor. We compare results from microbioreactor fermentations with *Escherichia coli* in which OD, DO, and pH are monitored continuously and compare these with results obtained in 500 mL bench-scale bioreactors. We present the results of off-line analysis of the medium to determine organic acid production and substrate utilization. We also present data on two different operating conditions within the microbioreactor to demonstrate the feasibility of obtaining statistically significant growth data from our system. Finally, we use modeling to understand the oxygen transfer characteristics of our microbioreactor and demonstrate that we can predict times for oxygen depletion and oxygen recovery based on growth characteristics of our model organism.

MATERIALS AND METHODS

Microbioreactor Fabrication

The microbioreactor (Fig. 1a) was fabricated out of poly(dimethylsiloxane) (PDMS) and glass. PDMS was used for the body of the fermenter, the bottom layer into which the sensors were sunk, and the aeration membrane. This polymer was selected for its biocompatibility, optical transparency in the visible range, and high permeability to gases (including oxygen and carbon dioxide) (Merkel et al., 2000). The base support of the bioreactor was made of glass, which provided the necessary rigidity as well as optical access. The typical volume of the microbioreactor was 5–50 μL, depending on the diameter used. The surface area-to-volume ratio was kept constant to ensure adequate oxygenation. The depth of the well was 300 μm, and the thickness of the aeration membrane was 100 μm. Of the experiments discussed below, those using complex medium were carried out in a volume of 5 μL, while those using defined medium were carried out in a volume of 50 μL to allow for off-line analysis of the medium.

The three PDMS layers were obtained by spincoating PDMS (Sylgard 184 Silicone Elastomer Kit, Dow Corning, Midland, MI) onto silanized silicon wafers to the required

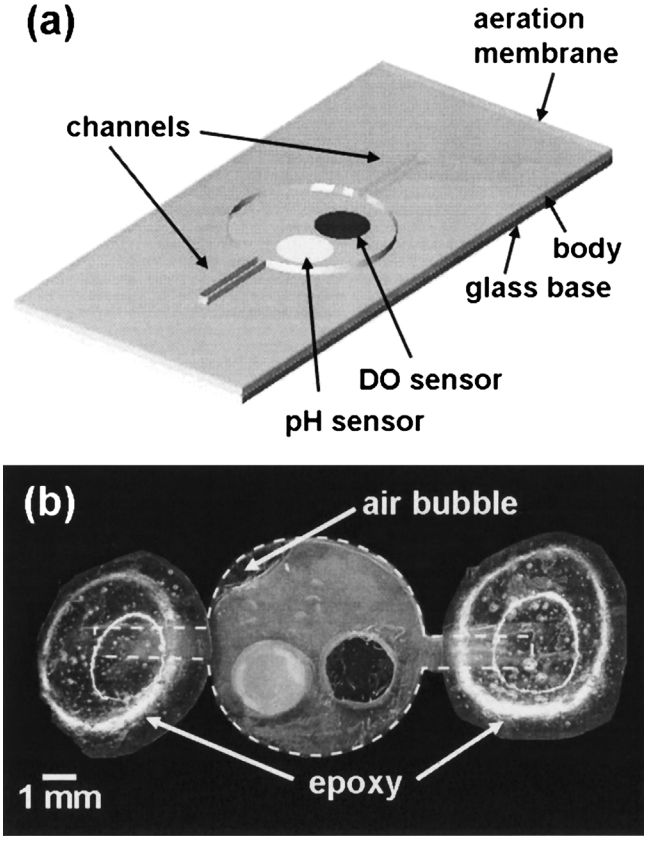

Figure 1. Microbioreactor built of three layers of PDMS on top of a layer of glass. (**a**) Solid model drawn to scale; (**b**) photograph of microbioreactor at the end of a run.

thickness. The PDMS was then cured for 2 h at 70°C, and the appropriate shapes were cut out of each layer. The bottom layer was 280 μm thick and contained two round holes into which two sensor foils were inserted, one for dissolved oxygen and one for pH, as described in the following section. Each sensor was 2 mm in diameter and 150–220 μm in height. The sensors were held in place with silicone vacuum grease. Recessing the foils in this way allowed the tops to be flush with the bottom of the microbioreactor, which is especially critical for the dissolved oxygen foil as a result of the oxygen gradient that develops in the medium during fermentations (see Results and Discussion). The 300-μm middle layer, which made up the body of the microbioreactor, consisted of a round opening of the desired diameter and channels for inoculation. The top layer was the 100-μm polymer aeration membrane. These layers were attached to each other and to the glass using an aquarium-grade silicone adhesive (ASI 502, American Sealants, Inc., Fort Wayne, IN) and allowed to cure overnight. Figure 1b shows a filled microbioreactor at the end of a fermentation run.

Analytical Methods

Optical sensing methods were selected to monitor biomass, dissolved oxygen, and pH. The major advantage of optical sensors is that the bulk of the cost and complexity of the sensing infrastructure can be kept outside of the microbioreactor, keeping the microbioreactor simple to fabricate, inexpensive, and thus disposable.

Optical density, calculated from a transmission measurement at 600 nm, was used to monitor biomass. Light from an orange LED (Epitex L600-10V, 600 nm, Kyoto, Japan) was passed through the microbioreactor, collected by a collimating lens (F230SMA-A, Thorlabs, Newton, NJ), and sent to a photodetector (PDA55, Thorlabs). The optical density was calculated using Eq. (1).

$$OD = 33.33\log_{10}\left(\frac{I_o}{I_{signal}}\right) \cdot \qquad (1)$$

In this equation, I_{signal} is the intensity of the signal and I_o is the intensity of the first measurement for a given experiment. Intensity readings were corrected for intensity fluctuations of the light source using a reference signal. The multiplication factor of 33.33 in Eq. (1) is a normalization for the path length of 300 μm in the microbioreactor which enables direct comparisons with results from conventional cuvettes with path lengths of 1 cm. This adjustment is only strictly valid if the absorption and light scattering by the cell culture are in the linear region. Calibration data from the microbioreactor using known concentrations of *E. coli* show that the measurements are within the linear region, i.e., before saturation is reached. It is important to note that this measurement is very sensitive to both the path length and to any curvature of the PDMS aeration membrane.

Fluorescence from oxygen- and pH-sensitive dyes was selected for the measurement of dissolved oxygen (Bacon and Demas, 1987; Klimant and Wolfbeis, 1995; Demas et al., 1999) and pH (Kosch et al., 1998; Lin, 2000), respectively, because of the high sensitivity and specificity of this measurement (Demas and DeGraff, 1991). The fluorescence of these dyes could be monitored using either fluorescence intensity or fluorescence lifetime measurements (Lakowicz, 1999). There are several major advantages to using lifetime measurements. They are insensitive to background light, fluctuations of the excitation source and photodetector, changes in distance from the excitation source, bending of optical fibers, changes in medium turbidity, leaching of the indicator, and displacement of the sensing layer relative to the measurement setup.

Both dissolved oxygen and pH were monitored by phase-modulation lifetime fluorimetry using commercially available sensor foils from PreSens Precision Sensing GmbH (Regensburg, Germany). Dissolved oxygen was measured using a PSt3 sensor foil, while pH was measured using an HP2A sensor foil.

Figure 2 shows the experimental setup. Bifurcated optical fibers (custom-made, RoMack Fiberoptics, Williamsburg, VA) connected to LEDs and photodetectors led into the chamber from both the top and bottom. As described above, a transmission measurement was used to calculate the optical density. The DO and pH sensors were excited with a square-wave modulated blue-green LED (NSPE590S, 505 nm, Nichia America Corporation, Mountville, PA) and a blue LED (NSPB500S, 465 nm, Nichia), respectively. Exciter bandpass filters (XF1016 and XF1014, Omega

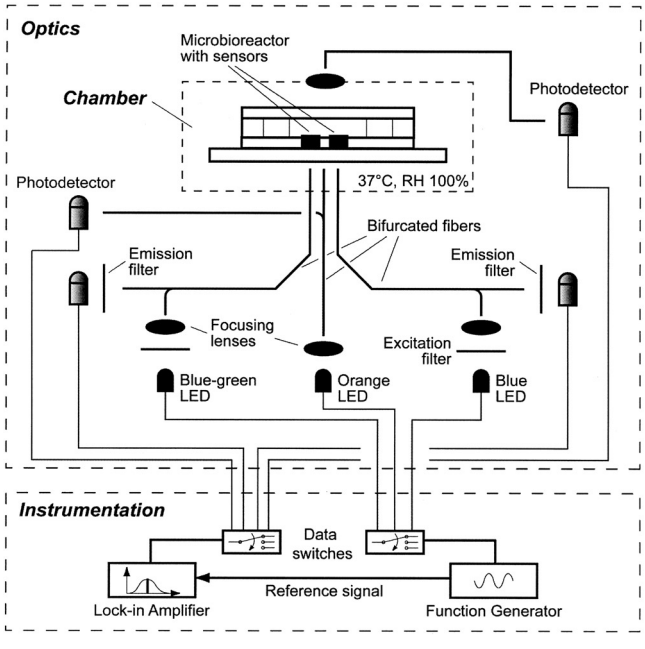

Figure 2. Schematic of the experimental setup. The chamber is kept at 100% humidity and 37°C. The microbioreactor is placed inside and the chamber is sealed. Three optical fibers carry three different wavelengths of light to the bottom of the microbioreactor for the three measurements: OD, DO, and pH. Photodetectors collect the transmitted or emitted light and send it to a lock-in amplifier where the signal is detected and analyzed.

Optical, Brattleboro, VT) and emission longpass filters (XF3016 and XF3018, Omega Optical) separated the respective excitation and emission signals and minimized cross-excitation. Data switches (8037, Electro Standards Laboratories, Cranston, RI) multiplexed the output signal and the input signal of the function generator (33120A, Agilent Technologies, Palo Alto, CA) and the lock-in amplifier (SR830, Stanford Research Systems, Sunnyvale, CA), respectively. The lock-in amplifier measured and output the phase shift, which is directly related to the fluorescence lifetime, between the excitation and emission signals for the DO and pH measurement. All instruments were PC-controlled under a LabVIEW software routine (National Instruments, Austin, TX), which allowed for automated and on-line measurement of the three parameters OD, DO, and pH. Readings of these parameters were taken every 10 min.

To determine the dissolved oxygen, the measured phase shift of the oxygen signal was related to the oxygen concentration using a modified Stern–Volmer equation (Carraway et al., 1991; Demas et al., 1995). An 11-point calibration between 0% and 100% oxygen was carried out to confirm the validity of the equation and to calculate a Stern–Volmer constant. It was found that a better fit was obtained for low oxygen concentrations when the calibration range included in the model fit was limited to 0–21% oxygen. Therefore, data from experiments with air as the contacting gas were processed using that range, while data from experiments using pure oxygen were processed using the full range of calibration.

The measured phase shift of the pH sensor fluorescence was related to the pH by fitting to the sigmoidal Boltzmann curve (Liebsch et al., 2001). A six-point calibration was carried out between pH 4 and 9 using colorless buffers (VWR International, West Chester, PA).

Microbioreactor Experimental Setup

Experiments were carried out in an airtight, aluminum chamber (Fig. 2). The chamber provided a means for controlling the humidity and the composition of the gas above the microbioreactor membrane. It also provided a large thermal mass for holding the temperature at the desired set point. The interior of the chamber had a volume that was large compared to the volume of the microbioreactor to ensure that gaseous oxygen was in large excess compared to the oxygen consumed by the cells during a fermentation. As a result, the chamber could be sealed for the duration of a run once it had been flushed with the desired gas. Temperature was controlled with a water bath that flowed water at the desired setpoint through the chamber base. Temperature was monitored using a thermocouple.

In addition to controlling environmental parameters, the chamber provided optical isolation and optical access for the desired measurements. Optical access was from the top and bottom of the chamber, directly above and below the microbioreactor, respectively, as shown in Fig. 2.

Biological Methodology

Organism and Medium

E. coli FB21591 (thiC::Tn5 -pKD46, Kan^R) was used in all experiments and obtained from the University of Wisconsin. Stock cultures were maintained at −80°C in 20% (vol/vol) glycerol. Prior to fermentation experiments, single colonies were prepared by streaking out the frozen cell suspension onto LB plates containing 2% (wt/vol) agar and 100 μg/mL of kanamycin. These plates were incubated overnight at 37°C to obtain single colonies, and subsequently stored in the refrigerator at 4°C for up to a week or used immediately to inoculate precultures.

Luria-Bertani medium was composed of 10 g/L tryptone (Difco Laboratories), 5 g/L yeast extract (Difco Laboratories, Detroit, MI), and 5 g/L NaCl. The solution was autoclaved for 40 min at 120°C and 150 kPa. The LB medium was supplemented with 10 g/L glucose (Mallinckrodt, Hazelwood, MO), 100 mM MES buffer at pH 6.9 (2-(*N*-morpholino)ethanesulfonic acid)) (Sigma), and 100 μg/mL of kanamycin (Sigma). The glucose stock solution was autoclaved for 20 min at 120°C and 150 kPa, and the MES and kanamycin stock solutions were filtered through 0.2-μm filters (Millipore, Billerica, MA).

The defined medium had the following composition: K_2HPO_4 [60 mM], NaH_2PO_4 [35 mM], $(NH_4)_2SO_4$ [15 mM], NH_4Cl [70 mM], $MgSO_4 \cdot 7H_2O$ [0.8 mM], $Ca(NO_3)_2 \cdot 4H_2O$ [0.06 mM], $FeCl_3$ [20 mM], MES [100 mM], glucose [10 g/L], thiamine [100 μM], kanamycin [100 μg/mL], $(NH_4)_6Mo_7O_{24} \cdot 4H_2O$ [0.003 μM], H_3BO_3 [0.4 μM], $CuSO_4 \cdot 5H_2O$ [0.01 μM], $MnCl_2 \cdot 4H_2O$ [0.08 μM], $ZnSO_4 \cdot 7H_2O$ [0.01 μM]. Glucose, MES, kanamycin, and thiamine were added to the medium as stock solutions.

Precultures

For experiments using LB medium, 5 mL of sterile medium were transferred into test tubes, and each was inoculated with a single colony of *E. coli* FB21591 from a LB–kanamycin agar plate. These cultures were incubated on a roller at 60 rpm and 37°C. Samples were removed periodically and measured for optical density (600 nm). When the optical density of the cultures reached OD = 1 ± 0.1, medium was removed from each test tube and transferred to a 500-mL baffled shake flask containing 30 mL of fresh medium to a starting optical density of 0.05. The inoculated shake flasks were incubated on shakers (150–200 rpm) at 37°C. Samples were withdrawn periodically until the optical density within the flasks reached OD = 1. At this point, the culture was used to inoculate either the bench-scale bioreactors or a microbioreactor.

Precultures for experiments using defined medium were carried out as above, except that the shake flasks into which the cultures from the test tubes were transferred contained defined medium.

Bench-Scale Bioreactor

Batch cultures were grown in 500-mL SixFors bioreactors (Infors, Switzerland) with a starting medium volume of 450 mL. Dissolved oxygen probes (405 DPAS-SC-K8S/200, Mettler Toledo, Toledo, OH) were calibrated with nitrogen gas (0% DO) and air (100% DO) prior to each run. pH probes (InPro 6100/220/S/N, Mettler Toledo) were calibrated with buffer at pH 7.0 and 4.0 (VWR).

The bioreactors were inoculated to a starting optical density of 0.05. The aeration rate of gas was set to 1 VVM (volume of gas per volume of medium per minute) and the impeller speed was set to 500 rpm. The k_La under these operating conditions, measured using the well-known method of "dynamic gassing out" (Van Suijdam et al., 1978), matched the k_La in the microbioreactor (measurement described in a later section). The temperature of the vessels was maintained at 37°C for all fermentations. Dissolved oxygen and pH were not controlled, so as to simulate the batch microbioreactor. The temperature, dissolved oxygen, and pH were recorded every 10 min throughout all fermentations. Biomass was monitored by removing samples from the bioreactor at defined time intervals and measuring the optical density at 600 nm on a spectrophotometer (Spectronic 20 Genesys, Spectronic Instruments, Leeds, U.K.).

Microbioreactor

Inoculation of the medium for the microbioreactor was carried out outside of the bioreactor. Ten milliliters of fresh medium was transferred to a Falcon conical tube, and to this was added the preculture medium from a shake flask for a starting optical density of 0.05. This inoculated medium was then introduced into the microbioreactor by injecting the liquid via channels (Fig. 1).

Sterility was maintained by the antibiotic kanamycin in the medium. Other methods of sterilizing, such as autoclaving and UV radiation, were not feasible due to the incompatibility of either the DO sensor or the pH sensor with each of these methods. Gamma radiation was tested as an alternative technique. Ethanol could also be used as a means of sterilization. However, for the present studies we found that using a fast-growing, antibiotic-resistant strain was sufficient for preventing contamination.

To ensure the flatness of the PDMS membrane, excess liquid was squeezed out of the chamber by applying a uniformly distributed pressure from the top. A bulge in the membrane would change the path length for the calculation of optical density, as well as change the distance over which diffusion of oxygen occurred, thus changing the mass transfer characteristics of the microbioreactor. After injection of the inoculated medium, the needle holes created in the channels were sealed with epoxy (Fig. 1). This was to prevent evaporation at these injection sites. Although PDMS self-seals to a large extent, we have noticed that needle holes increase the rate of evaporation and provide sites for the growth of air bubbles.

Once the microbioreactor was filled with medium it was placed inside the chamber and secured to the base. Open reservoirs of water were placed inside the chamber to provide humidity. Keeping the atmosphere within the chamber at high humidity minimizes evaporative losses through the PDMS membrane. The chamber was then closed, and continuous readings were started. When fermentations were performed with pure oxygen in the chamber headspace, oxygen was passed through the chamber prior to the start of the readings.

The time between inoculation of fresh medium and placement of the filled microbioreactor in the chamber was 20 min. During this time, the medium was kept at room temperature to minimize cell growth. The time between placement of the bioreactor in the chamber and the first reading was 10 min. During this time, the bioreactor and cells warmed up to 37°C.

Cell Counts

Estimates of cell titer from the microbioreactor and the bench-scale bioreactor were obtained using two methods. Direct cell counts were carried out using a Petroff–Hausser counting chamber and standard counting methodology. Viable cell counts were carried out using the technique of plating serial dilutions (Ausubel et al., 1995).

Medium Analysis

A series of experiments in defined medium was carried out to provide samples for off-line analysis of organic acids and glucose in both the bench-scale bioreactor and the microbioreactor.

During fermentations in the bench-scale bioreactors, samples of the medium were periodically removed, filtered, and frozen for later analysis.

Samples from the microbioreactors were obtained by sacrificing their entire volume. In order to obtain a sufficient volume of medium for analysis, the microbioreactors were fabricated to contain a volume of 50 μL. This allowed for volume loss during filtering and transfers, and provided sufficient filtered volume to meet the requirements of the HPLC protocol (5 μL). The medium samples were collected over several days. Each day, three microbioreactors were inoculated and allowed to run in parallel while process parameters were measured. All three were then sacrificed at a predetermined time, and their contents were removed, filtered, and frozen. In this way, microbioreactor data was obtained at five time points.

An Agilent 1100 Series HPLC equipped with an organic acid analysis column (Aminex HPX-87H ion exclusion column, Bio-Rad, Hercules, CA) was used for off-line medium analysis. Samples were prepared by filtration through a

0.2-μm membrane (Pall Gelman Laboratory, East Hills, NY). Calibration was carried out by running standards at two concentrations for each of the organic acids assayed, and four different standards for glucose. A linear fit through the origin was obtained for all of the concentration ranges used.

Table II. List of variables used in models.

Variable	Description
C	Concentration of oxygen
D	Diffusivity of O_2 in each phase
R_V	Volumetric accumulation term
N	Number of cells
μ	Specific growth rate of cells
k_La	Oxygen transfer coefficient

RESULTS AND DISCUSSION

Modeling of Oxygen Transport and Consumption

The design of the microbioreactor was based on preliminary modeling of the oxygen transfer through the PDMS membrane and the medium using the simulation software FEMLAB (parameters used are listed in Table I, variables used are listed in Table II). Monod growth (Monod, 1949) of homogeneously dispersed cells with oxygen as the limiting substrate was assumed. The Monod constant was approximated by using the critical oxygen concentration for *E. coli* (Bailey and Ollis, 1986). R_V was zero within the membrane.

$$\frac{\partial C}{\partial t} = D\frac{\partial^2 C}{\partial x^2} - R_v, \tag{2}$$

$$R_v = \text{Oxygen Uptake Rate} = -Y_{O/X}\frac{dN}{dt}, \tag{3}$$

$$\frac{dN}{dt} = N\mu, \tag{4}$$

$$\mu = \frac{\mu_{\max} C}{K_S + C}. \tag{5}$$

We determined that a depth of 300 μm allowed sufficient oxygenation for a final cell number of $\sim 10^9$ cells/mL to be obtained. It was found that the major resistance to mass transfer occurs in the medium rather than the membrane, a result of the low solubility of oxygen in water. From the model, it is also evident that a concentration gradient exists within the medium as oxygen is gradually depleted. Oxygen depletion occurs first at the bottom and moves gradually up the microbioreactor. This is shown in the cross-sectional view of Fig. 3, which shows oxygen concentration as a function of depth at increasing time.

Because of the presence of the oxygen gradient, the height of the dissolved oxygen sensor foil is critical to the measurements obtained. If the sensor is raised above the height of the microbioreactor bottom or is somehow at an angle, it will take longer to be reached by the zero-dissolved-oxygen zone during depletion and will register dissolved oxygen earlier during reoxygenation of the medium. Depending on its height, it may never show oxygen depletion. Thus the oxygen sensor must be positioned such that its entire surface is exposed to the same oxygen concentration. In this case, the gradient is perpendicular to the bottom of the fermenter, and the foil must then be positioned horizontally (i.e., along the bottom of the chamber), rather than on the side where readings would be ambiguous.

Oxygen depletion occurs after approximately 3 h at the bottom of the microbioreactor (Fig. 4). Experimental data show a similar trend. The model has also been used to successfully predict dissolved oxygen curves for *E. coli* growing

Table I. List of parameters used in models.

Parameter	Definition	Value	Reference
S_{PDMS}	Solubility of O_2 in PDMS[a]	0.18 cm^3(STP)/cm^3·atm	Merkel et al., 2000
D_{PDMS}	Diffusivity of O_2 in PDMS[a]	3.4×10^{-5} cm^2/s	Merkel et al., 2000
S_{H_2O}	Solubility of O_2 in water[a,b]	7.36 mg/L	Perry and Green, 1984
D_{H_2O}	Diffusivity of O_2 in water[a,b]	2.5×10^{-5} cm^2/s	Perry and Green, 1984
K	PDMS-H_2O partition coefficient[a,b]	0.135	Calculated
$Y_{O/X}$	Yield of biomass on oxygen	1 g_{O2} consumed/g_{DCW} (dry cell weight) produced	Konz et al., 1998
N_0	Initial number of cells	3.8×10^7 cells/mL	Experiment
t_d	Doubling time	30 min	Experiment
μ_{max}	Maximum specific growth rate	0.0231 min^{-1}	Experiment
	Conversion	5.5×10^{-13} g_{DCW}/*E. coli* cell	Experiment
K_s	Monod constant[c]	0.26 mg/L	Calculated
k	Logistic model constant	0.025	Model fit
β	Logistic model constant	2.5×10^{-16} m^3/cell	Model fit
C^c	Percent oxygen at saturation	100%	Definition

[a]At 35°C, in equilibrium with 0.21 atm of oxygen.
[b]Values for pure water were used because 10 g/L of glucose was present in the medium.
[c]Critical oxygen concentration = 0.0082 mmol/L ($\sim$3.6% of air saturation) (Bailey and Ollis, 1986).

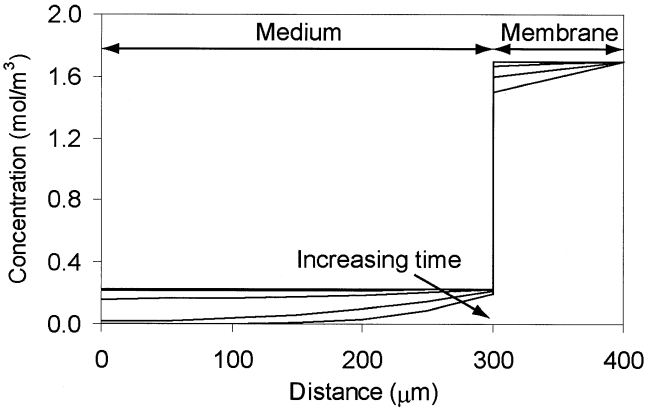

Figure 3. Modeled oxygen gradient within the medium and the membrane of the microbioreactor. Monod growth was assumed. Oxygen concentrations are shown at t = 0, 0.5, 1, 1.5, and 2 h.

in defined medium. During bacterial growth, the oxygen-depletion phase typically corresponds to the period of biomass increase as measured by optical density. After some time, the cells enter stationary phase, at which time metabolism shifts from growth to maintenance. Oxygen demand drops significantly, allowing oxygen levels to recover.

To model this oxygen recovery observed in experiments, the logistic curve [Eq. (6)] was fit to experimental growth data and substituted for N in Eq. (3). This model was developed by Verhulst (1838) to describe population growth and includes cell concentration-dependent inhibition. As in the case of the Monod model, this simple model is both unstructured (balanced growth approximation) and unsegregated ("average cell" approximation). It is useful when the limiting nutrient is unknown or when multiple factors affect cellular growth, as is the case here. To take these multiple factors into account would necessitate the removal of the balanced-growth assumption listed above and a move toward structured models, which is not the major focus of this paper. The logistic model is therefore used despite its limitations. The fit to the curve is shown in Fig. 5a.

$$N = \frac{N_o e^{kt}}{1 - \beta N_o (1 - e^{kt})}. \quad (6)$$

Modeling of the oxygen concentration within the microbioreactor using this fit is shown in Fig. 5b. The difference between the predicted and measured curves in Fig. 5 may be attributed to the limitations of the model used, as discussed above.

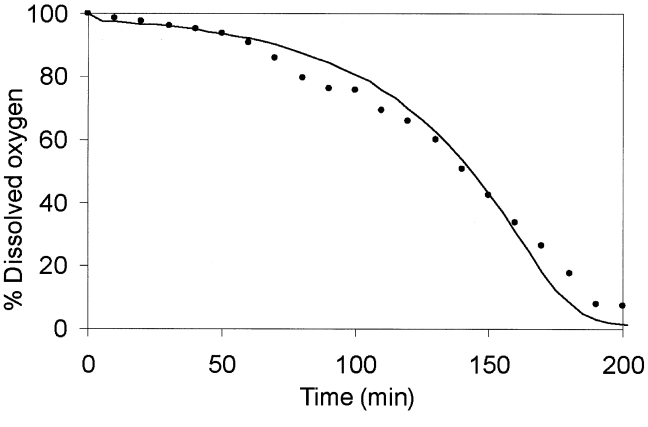

Figure 4. Oxygen concentration at the bottom of the microbioreactor during a fermentation as a function of time when the doubling time is 30 min. Model (—) uses Monod growth to predict oxygen depletion, experimental data (●) is for a fermentation run with a resulting doubling time of 30 min.

Mass Transfer Coefficient

To allow the comparison of results obtained with the microbioreactor and the bench-scale reactor, a value of $k_L a$ was measured in the microbioreactor and the operating conditions of the larger bioreactor were set so that its $k_L a$ value would be comparable. The calculation of the $k_L a$ in the microbioreactor was based on a kinetic experiment (at 37°C) in which the medium was allowed to come to

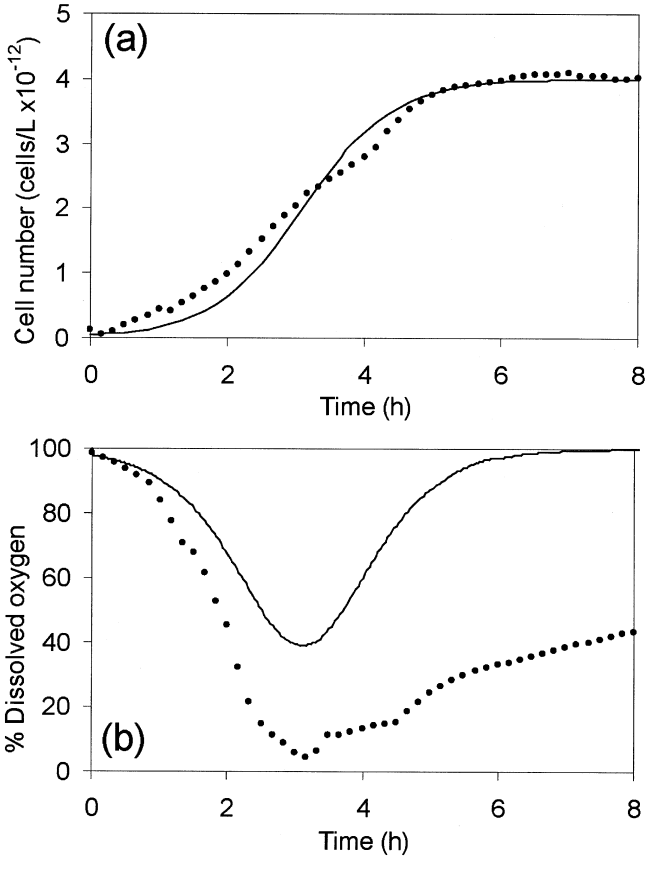

Figure 5. (**a**) Logistic curve (—) fit to experimental data (●) with k = 0.025, $\beta = 2.5 \times 10^{-16}$ m^3/cell. Experimental data is an average of three fermentations. (**b**) Oxygen concentration at the bottom of the microbioreactor over time during a fermentation. Theoretical curve (—) uses a logistic model for cell growth, experimental data (●) is an average of three fermentations.

equilibrium with nitrogen (0% DO) in the chamber headspace, at which time the headspace was flushed with air (100% DO) and continuous readings of the dissolved oxygen at the bottom of the microbioreactor were taken. Except for the absence of active stirring, this technique is similar to that of the dynamic "gassing-out" method that is commonly used for stirred bioreactors, during which the k_La is extracted as a first-order rate constant using Eq. (7). This technique has previously been used to find the k_La of a stagnant system (Randers-Eichhorn et al., 1996).

$$\frac{dC}{dt} = k_La(C^* - C). \tag{7}$$

The first-order approximation of Eq. (7) is applicable if mass transfer is slow relative to the response time of the sensor. If the time response of the sensor is potentially significant relative to that of the entire system, a second-order fit can be used as in Eq. (8), where τ_1 is the time constant of the sensor and τ_2 is the time constant of mass transfer:

$$C(t) = 100\left(1 - \frac{\tau_1 e^{-\frac{t}{\tau_1}} - \tau_2 e^{-\frac{t}{\tau_2}}}{\tau_1 - \tau_2}\right). \tag{8}$$

Experimentally we found the time constant of our sensor to be $\sim$5 s. When response curves of our system were fit to Eq. (8), we calculated an average k_La of $\sim$60 h^{-1}. This is within the range of values measured in shake flasks (Maier and Buchs, 2001; Gupta and Rao, 2003; Wittmann et al., 2003) and shaken microtiter plates (Hermann et al., 2003; John et al., 2003b).

We carried out a dynamic simulation of the experimental setup and procedure using FEMLAB (The MathWorks, Inc., Natick, MA). In the simulation we modeled the two-level microbioreactor inside the chamber, through which air flowed at the measured flow rate starting at $t = 0$. The initial conditions imposed were 0% oxygen concentration within the medium and in the membrane. The resulting oxygen curve yielded $k_La \sim 170\ h^{-1}$ ($\tau \sim 21$ s). The flow rate of air through the chamber was high enough that any boundary layer formed at the air–membrane interface was negligible.

The discrepancy between the measured and theoretical time constants for this system may be a result of assumptions made about the permeability of the PDMS membrane. It can be shown that any decrease in the solubility or diffusivity of oxygen in PDMS that is used in the model will have a large impact on the calculated k_La, which is extracted from a fast process (time scale of tens of seconds), while having little impact on the oxygen transfer during a fermentation, which is a slow process (time scale of hours) during which the PDMS presents relatively little transport resistance. This difference in the permeability could either be due to experimental conditions, such as the age of the membrane or the presence of oil or dust on the surface, or simply a difference between the PDMS used in experiments and that reported in literature (such as degree of cross-linking).

It should also be noted that the method of fitting a curve to the oxygen concentration on the bottom of the microbioreactor to estimate a k_La provides a lower bound for the measurement, since this is where the lowest concentration of oxygen is found at every time point. The extracted k_La will be larger if, for example, a space-average of the oxygen concentration is used. For the case of the simulation, with which $\tau \sim 21$ s ($k_La \sim 170\ h^{-1}$) was calculated using the bottom DO level, taking a space-average of the DO and finding the time constant of the resulting response curve yields $\tau \sim 14$ s ($k_La \sim 250\ h^{-1}$).

Fermentations With Air

Experiments in defined medium were carried out in both the microbioreactors and the bench-scale bioreactors. MES buffer was added to provide some stabilization for the pH, since pH control was not implemented. The objectives were to establish the reproducibility of the microbioreactor relative to the bench-scale, and to demonstrate the feasibility of time-point sacrificing of the microbioreactors in order to carry out off-line analysis of the bioreactor medium throughout a fermentation. Three microbioreactors were sacrificed at each time point, and the medium was analyzed for glucose consumption and mixed-acid fermentation products using HPLC. In basic research or scale-up applications, this type of analysis would be necessary if an in situ sensor was not available for an analyte of interest.

The three measured parameters within the microbioreactor and the bench-scale bioreactor are shown in Fig. 6. Each curve represents a separate run. Comparison of Figs. 6a and b shows that the optical density in both bioreactor types displays a similar trend, and results in a similar final OD of $\sim$6.

Figures 6c and d show the dissolved oxygen as a function of time in the microbioreactor and the bench-scale bioreactor, respectively. Again, it can be seen that the trend in both bioreactors is similar, even though the SixFors chambers are mixed. This result is consistent with the similar values of oxygen mass transfer (k_La) for the two systems. Oxygen levels deplete during the exponential growth of cultures and eventually recover as the bacteria reach stationary phase.

The trends for pH variation over time within both bioreactor types are again very similar. It appears that this measurement exhibits less variation between runs in the microbioreactor than the DO measurement. This is most likely due to the insensitivity of the pH measurement to the positioning of the pH sensor, suggesting that a pH gradient does not exist within the microbioreactor and the bioreactor can be considered well-mixed with respect to protons.

This was confirmed experimentally by placing the pH sensor at the top of the chamber during a fermentation run. The pH curve showed the same time profile as those from fermentations in which the sensor was at the bottom. This result is consistent with the analysis of the reaction and

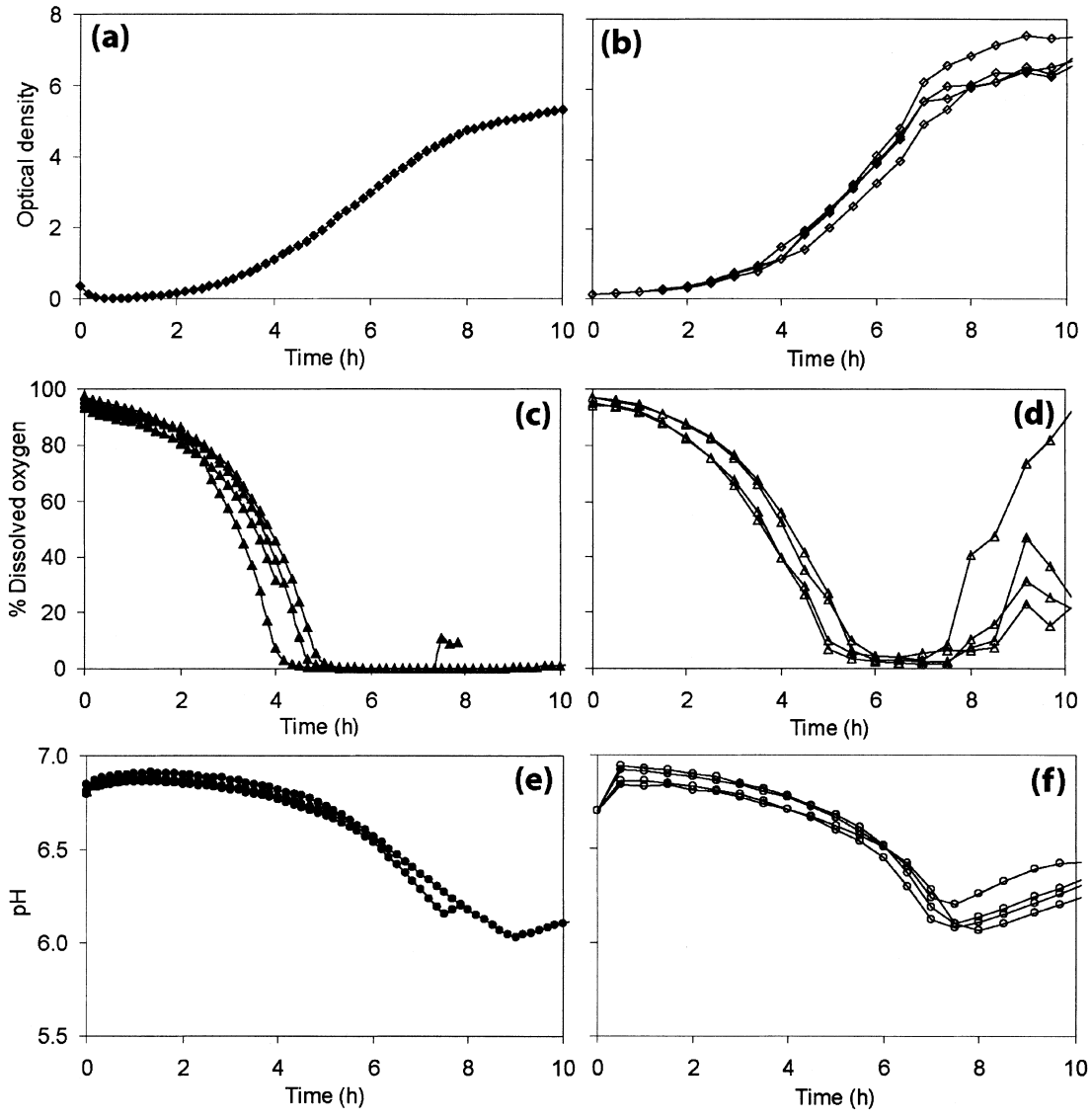

Figure 6. Replicate fermentations with *E. coli* in defined medium in the microbioreactor and a bench-scale bioreactor: (**a**) OD in microbioreactor; (**b**) OD in bench-scale bioreactor; (**c**) DO in microbioreactor; (**d**) DO in bench-scale bioreactor; (**e**) pH in microbioreactor; (**f**) pH in bench-scale bioreactor. Experiments in the microbioreactor were performed on successive days, and microbioreactors were sacrificed each day at a predetermined time. The medium was harvested for HPLC analysis. Each data series represents a single run.

diffusion times within the microbioreactor. An estimate of the reaction time can be obtained by converting the pH versus time curve to an $[H_3O^+]$ versus time curve. The steepest slope on this curve can be used to find the largest $d[H_3O^+]/dt/(\sim 5 \times 10^{-9}$ M/min). Normalizing this slope with the concentration of H_3O^+ at that time point ($\sim 5 \times 10^{-7}$ M) gives a $t_{rxn} \sim 100$ min. Note, this is not the time scale for the acid–base reaction, which is very rapid, but the time scale for the pH change as a result of the growth. The diffusion time of the system with respect to protons can be estimated as L^2/D, where L is the distance over which diffusion occurs and D is the diffusion coefficient. Using $D_H^+ = 9.311 \times 10^{-5}$ cm^2/s (at 25°C) (Lide, 2001) gives $t_{diff} \sim 0.2$ min. Thus, $t_{rxn} \gg t_{diff}$ implying that a pH gradient would not be expected and the pH sensor would not be affected by its location in the microbioreactor, as observed experimentally.

When bacteria were viewed at the end of fermentation runs, the morphology of all cultures looked normal, with no stress-induced elongation visible. Final direct cell counts in both bioreactor types were carried out, and the concentration of cells in each was found to be on the order of 10^9 cells/mL. This estimate is consistent with the numbers obtained from viable cell counts, which yielded counts of $(1–4) \times 10^9$ CFU/mL in both sizes of bioreactor.

Figure 7 shows concentration curves for the analytes measured using HPLC. The glucose uptake in the microbioreactor (Fig. 7a) corresponds closely with that in the larger bioreactor. Additionally, Fig. 7b shows that concentrations of the *E. coli* mixed-acid fermentation products

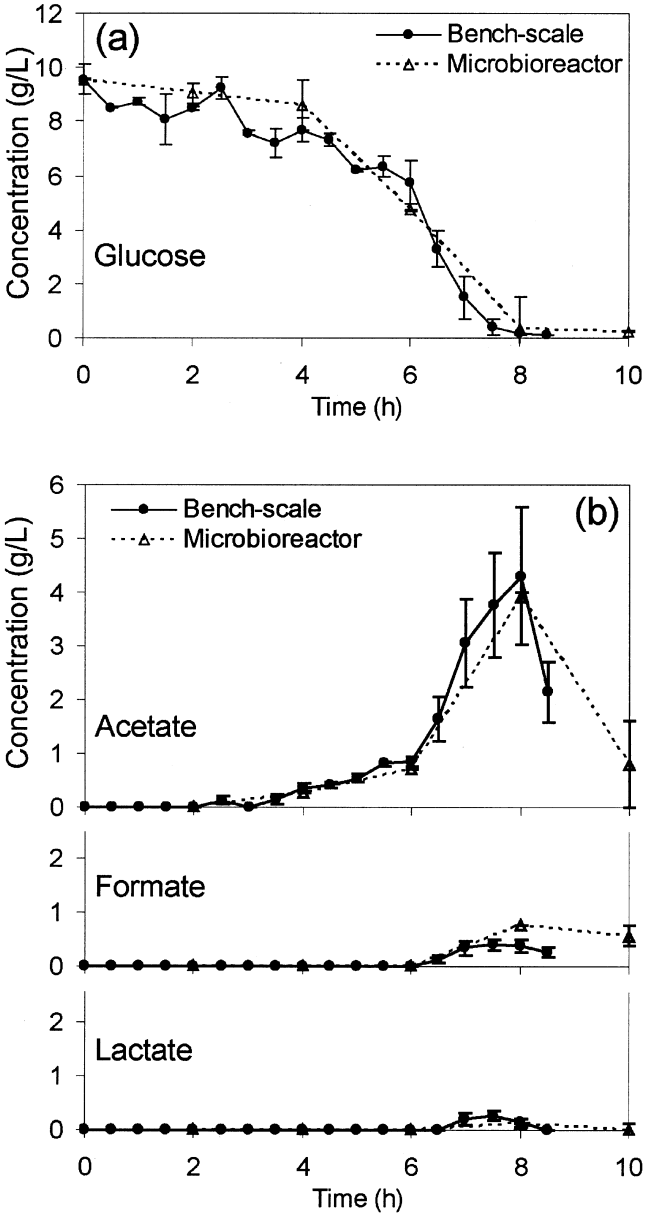

Figure 7. (**a**) Glucose uptake during fermentations with *E. coli* in defined medium in a bench-scale bioreactor ($n = 2$) and a microbioreactor ($n = 3$). Data is averaged over n runs, error bars report standard error. (**b**) Organic acid production during fermentations of *E. coli* in defined medium in a bench-scale bioreactor ($n = 4$) and a microbioreactor ($n = 3$). Data is averaged over n runs, error bars report standard error.

acetate, formate, and lactate show similar trends in both bioreactor systems (succinate was not found in either bioreactor type). Acetate in particular is produced in significant amounts as the fermentation proceeds.

Fermentations With Pure Oxygen

Additional experiments were carried out in LB medium, with air and 100% oxygen in the headspace of the chamber (above the aeration membrane) to determine whether a difference could be observed in bacterial growth characteristics. Supplying a partial pressure of 1 atm of oxygen above the microbioreactor leads to an approximate 5-fold increase in the solubility of oxygen in the medium, as defined by Henry's law. This approach is commonly used in large-scale fermentations to avoid oxygen limitations. An extensive literature exists on the effects of total and partial oxygen pressure on microorganisms, including *E. coli*. (Brunker and Brown, 1971; Gottlieb, 1971; Konz et al., 1998). The general consensus appears to be that partial pressures of oxygen higher than those found in air are toxic to microorganisms and inhibit their growth, but that this effect is less pronounced in a robust organism such as *E. coli*. Growth inhibition has been noted in *E. coli* in the presence of pure oxygen when minimal medium is used. It is thought that the absence of CO_2 contributes to this inhibition (Onken and Liefke, 1989). Although it is known that CO_2 can inhibit microbial growth, some CO_2 may be needed by a culture growing in minimal medium for the biosynthesis of essential compounds. In a complex medium, these compounds may already be present. Alternatively, fermentation of substrates within the complex medium may provide sufficient CO_2 to meet the needs of the cells. In either case, the lack of CO_2 is not inhibitory. As a result, *E. coli* grown in rich medium under pure oxygen conditions does not seem to show inhibited growth. The focus of the present microbioreactor study was the effect of increased oxygen levels on *E. coli* growth.

In the presence of pure oxygen the initial maximum growth rate (Fig. 8a) does not appear to be different than the growth rate in the presence of air, but the bacteria are able to maintain it for a longer period of time. This is supported by the calculated doubling time in each case. With air in the headspace $t_d = 28$ min $\pm$ 3 min, and with oxygen in the headspace $t_d = 24$ min $\pm$ 6 min. The overlapping error bars indicate that the difference in the mean is not statistically significant (at one standard error). The maximum optical density (and thus cell count) is somewhat higher when pure oxygen is used compared to air. As stationary phase progresses, however, the optical density of cells under pure oxygen decreases until the curve coincides with the air curve. This effect could possibly be attributed to higher rates of cell lysis under pure oxygen conditions.

When pure oxygen is contacted with the aeration membrane (Fig. 8b), the oxygen within the medium shows a minimum but never depletes entirely. The minimum oxygen level that the bacteria encounter is approximately 70%. This oxygen level is still three times higher than the maximum oxygen level with air as the contacting gas. In the case of the pH time course within the microbioreactor (Fig. 8c), the error bars, representing standard error, do not show overlap at any time point beyond the beginning of the fermentation. The curves show that the pH experiences a sharper drop in the presence of oxygen than in the presence of air. This is consistent with the higher growth observed in the OD curve in the presence of pure oxygen. Because the major source of protons in the medium comes from the protons that are excluded as ammonia (existing as NH_4^+ in the medium) crosses the cell membrane and is internalized as NH_3 (Bauer and

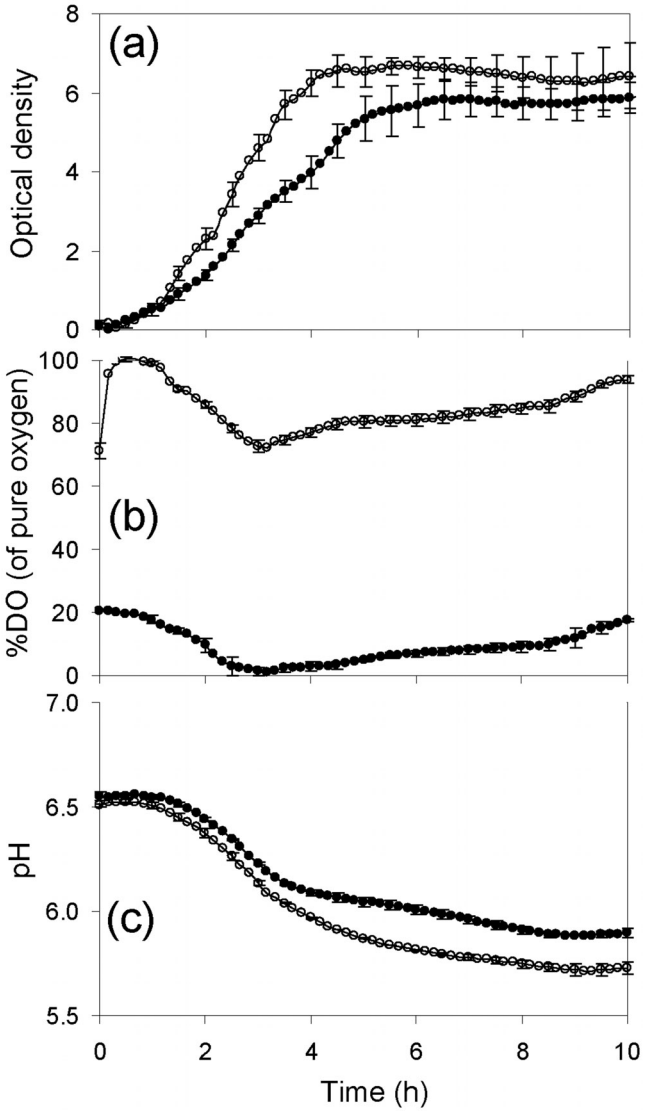

Figure 8. Comparison of (**a**) optical density, (**b**) dissolved oxygen, and (**c**) pH with *E. coli* grown in LB medium in a microbioreactor with air ($n = 3$) and oxygen ($n = 3$) in chamber headspace. Data is averaged over n runs, error bars report standard error. (○), oxygen. (●), air.

Shiloach, 1974), more growth would be expected to lead to a higher rate of proton generation and, subsequently, a lower pH. At the end of fermentation runs with oxygen, bacteria exhibit normal morphology.

CONCLUSIONS

We have demonstrated the operation of a microbioreactor with a volume as low as 5 μL containing integrated, automated sensors for the measurement of OD, DO, and pH. We have shown that results from the microbioreactor are reproducible in both rich medium (LB) and defined medium, and that we are able to understand the oxygen transfer characteristics of the microbioreactor and effectively model growth and oxygen consumption of the bacteria during a fermentation. We have also shown that it is possible to sequentially sacrifice microbioreactors that are running in parallel to carry out off-line analysis using traditional techniques. Finally, we have shown that results obtained from the microbioreactor correspond closely with results obtained in bench-scale volumes. This suggests that our microbioreactor can effectively bridge the gap between current high-throughput processes that yield little data, such as microtiter plates, and scale-up to increasingly large bioreactors that approach production scale. In effect, microbioreactors have the potential to provide much of the data and functionality that a large bioreactor system makes available while offering the advantages of high-throughput processes, in terms of labor, time, and cost.

Future work on the microbioreactor bioprocessing platform will need to address integration and streamlining of the fluid handling. In particular, the incubation and preculture stages are both time- and labor-intensive. The ability to go from inoculation with cells from a plate to a completed fermentation run on a single device would greatly reduce both the effort involved in preparing for and running fermentations as well as the sources of error associated with current transfers between stages. Future efforts should also involve the integration of additional sensors into the microbioreactor. In particular, a sensor for the measurement of CO_2 is desirable (Ge et al., 2003). The ability to measure the level of CO_2 in the medium as well as the off-gas would allow the closing of the carbon balance on the system. This would enable experiments such as isotopic studies and flux analyses to be carried out on a large scale with minimal quantities of reagent.

We gratefully acknowledge the DuPont–MIT Alliance (DMA) for funding and the Swiss National Foundation for additional funding. The authors thank Nathalie Gorret and members of the DuPont Company for stimulating discussions about bioreactors.

References

Anderlei T, Buchs J. 2001. Device for sterile online measurement of the oxygen transfer rate in shaking flasks. Biochemical Engineering Journal 7(2):157–162.

Ausubel FM, Brent R, Kingston RE, Moore DD, Seidman JG, Smith JA, Struhl K (editors). 1995. Short protocols in molecular biology, 3rd edition. New York: John Wiley & Sons, Inc.

Bacon JR, Demas JN. 1987. Determination of oxygen concentrations by luminescence quenching of a polymer-immobilized transition-metal complex. Anal Chem 59(23):2780–2785.

Bailey JE, Ollis DF. 1986. Biochemical engineering fundamentals. New York: McGraw-Hill, Inc.

Bauer S, Shiloach J. 1974. Maximal exponential growth rate and yield of *E. coli* obtainable in a bench-scale fermentor. Biotechnol Bioeng 16(7):933–941.

Brunker RL, Brown OR. 1971. Effects of hyperoxia on oxidized and reduced NAD and NADP concentrations in *Escherichia coli*. Microbios 4(15):193–203.

Carraway ER, Demas JN, DeGraff BA, Bacon JR. 1991. Photophysics and photochemistry of oxygen sensors based on luminescent transition-metal complexes. Anal Chem 63(4):337–342.

Chartrain M, Salmon PM, Robinson DK, Buckland BC. 2000. Metabolic

engineering and directed evolution for the production of pharmaceuticals. Curr Opin Biotechnol 11(2):209–214.
Demas JN, DeGraff BA. 1991. Design and applications of highly luminescent transition metal complexes. Anal Chem 63(17):829–837.
Demas JN, DeGraff BA, Xu W. 1995. Modeling of luminescence quenching-based sensors: comparison of multisite and nonlinear gas solubility models. Anal Chem 67(8):1377–1380.
Demas JN, DeGraff BA, Coleman PB. 1999. Oxygen sensors based on luminescence quenching. Anal Chem 71(23):793A–800A.
Ge X, Kostov Y, Rao G. 2003. High-stability non-invasive autoclavable naked optical CO_2 sensor. Biosens Bioelectron 18(7):857–865.
Gottlieb SF. 1971. Effect of hyperbaric oxygen on microorganisms. Annu Rev Microbiol 25:111–152.
Gram A. 1997. Biochemical engineering and industry. J Biotechnol 59 (1–2):19–23.
Gupta A, Rao G. 2003. A study of oxygen transfer in shake flasks using a non-invasive oxygen sensor. Biotechnol Bioeng 84(3):351–358.
Hermann R, Lehmann M, Buchs J. 2003. Characterization of gas–liquid mass transfer phenomena in microtiter plates. Biotechnol Bioeng 81(2):178–186.
John GT, Goelling D, Klimant I, Schneider H, Heinzle E. 2003a. pH-Sensing 96-well microtitre plates for the characterization of acid production by dairy starter cultures. J Dairy Res 70(3):327–333.
John GT, Klimant I, Wittmann C, Heinzle E. 2003b. Integrated optical sensing of dissolved oxygen in microtiter plates: a novel tool for microbial cultivation. Biotechnol Bioeng 81(7):829–836.
Kim JW, Lee YH. 1998. Development of microfermenter chip. J Korean Phys Soc 33:S462–S466.
Klimant I, Wolfbeis OS. 1995. Oxygen-sensitive luminescent materials based on silicone-soluble ruthenium diimine complexes. Anal Chem 67(18):3160–3166.
Konz JO, King J, Cooney CL. 1998. Effects of oxygen on recombinant protein expression. Biotechnol Prog 14(3):393–409.
Kosch U, Klimant I, Werner T, Wolfbeis OS. 1998. Strategies to design pH optodes with luminescence decay times in the microsecond time regime. Anal Chem 70(18):3892–3897.
Kostov Y, Harms P, Randers-Eichhorn L, Rao G. 2001. Low-cost microbioreactor for high-throughput bioprocessing. Biotechnol Bioeng 72(3):346–352.
Lakowicz JR, editor. 1999. Principles of fluorescence spectroscopy, 2nd edition. New York: Plenum Publishing Corporation.
Lamping SR, Zhang H, Allen B, Shamlou PA. 2003. Design of a prototype miniature bioreactor for high throughput automated bioprocessing. Chem Eng Sci 58(3–6):747–758.
Lide DR (editor). 2001. CRC handbook of chemistry and physics, 82nd edition. Boca Raton, FL: CRC Press.
Liebsch G, Klimant I, Krause C, Wolfbeis OS. 2001. Fluorescent imaging of pH with optical sensors using time domain dual lifetime referencing. Anal Chem 73(17):4354–4363.
Lin J. 2000. Recent development and applications of optical and fiber-optic pH sensors. TRAC—Trends Anal Chem 19(9):541–552.
Maharbiz MM, Holtz WJ, Howe RT, Keasling JD. 2004. Microbioreactor arrays with parametric control for high-throughput experimentation. Biotechnol Bioeng 85(4):376–381.
Maharbiz MM, Holtz WJ, Sharifzadeh S, Keasling JD, Howe RT. 2003. A microfabricated electrochemical oxygen generator for high-density cell culture arrays. J Microelectromech Syst 12(5):590–599.
Maier U, Buchs J. 2001. Characterisation of the gas-liquid mass transfer in shaking bioreactors. Biochem Eng J 7(2):99–106.
Merkel TC, Bondar VI, Nagai K, Freeman BD, Pinnau I. 2000. Gas sorption, diffusion, and permeation in poly(dimethylsiloxane). J Polym Sc Pt B-Polym Phys 38(3):415–434.
Monod J. 1949. The growth of bacterial cultures. Annu Rev Microbiol 3:371–394.
Onken U, Liefke E. 1989. Effect of total and partial pressure (oxygen and carbon dioxide) on aerobic microbial processes. Adv Biochem Eng/Biotechnol (Bioproc Eng) 40:137–169.
Parekh S, Vinci VA, Strobel RJ. 2000. Improvement of microbial strains and fermentation processes. Appl Microbiol Biotechnol 54(3): 287–301.
Perry RH, Green D (editors). 1984. Perry's chemical engineering handbook. Chicago: R. R. Donnelley & Sons Company.
Randers-Eichhorn L, Bartlett RA, Frey DD, Rao G. 1996. Noninvasive oxygen measurements and mass transfer considerations in tissue culture flasks. Biotechnol Bioeng 51(4):466–478.
Schmid RD, Hammelehle R. 2003. Pocket guide to biotechnology and genetic engineering. New York: Wiley-VCH.
Shanks JV, Stephanopoulos G. 2000. Biochemical engineering—bridging the gap between gene and product. Curr Opin Biotechnol 11:169–170.
Stitt DT, Nagar MS, Haq TA, Timmins MR. 2002. Determination of growth rate of microorganisms in broth from oxygen-sensitive fluorescence plate reader measurements. BioTechniques 32(3):684–689.
Tolosa L, Kostov Y, Harms P, Rao G. 2002. Noninvasive measurement of dissolved oxygen in shake flasks. Biotechnol Bioeng 80(5):594–597.
Van Suijdam JC, Kossen NWF, Joha AC. 1978. Model for oxygen transfer in a shake flask. Biotechnol Bioeng 20(11):1695–1709.
Verhulst P-F. 1838. Notice sur la loi que la population suit dans son accroissement. Corresp Math Phys 10:113–121.
Weuster-Botz D, Altenbach-Rehm J, Arnold M. 2001. Parallel substrate feeding and pH-control in shaking-flasks. Biochem Eng J 7(2): 163–170.
Wittmann C, Kim HM, John G, Heinzle E. 2003. Characterization and application of an optical sensor for quantification of dissolved O_2 in shake-flasks. Biotechnol Lett 25(5):377–380.